μ-Conotoxin SmIIIA, a Potent Inhibitor of Tetrodotoxin-Resistant Sodium Channels in Amphibian Sympathetic and Sensory Neurons†

Peter J. West,[‡,§] Grzegorz Bulaj,[§,||] James E. Garrett,[||] Baldomero M. Olivera,[§] and Doju Yoshikami*[,§]

Interdepartmental Program in Neuroscience and Department of Biology, University of Utah, Salt Lake City, Utah 84112, and Cognetix, Inc., 421 Wakara Way, Salt Lake City, Utah 84108

Received August 2, 2002; Revised Manuscript Received October 16, 2002

ABSTRACT: μ-Conotoxins are a family of peptides from the venoms of predatory cone snails. Previously characterized μ-conotoxins preferentially block skeletal muscle voltage-gated sodium channels. We report here the discovery (via cloning), synthesis, and electrophysiological characterization of a new peptide in this family, μ-conotoxin SmIIIA from *Conus stercusmuscarum*. Although μ-conotoxin SmIIIA shares several biochemical characteristics with other μ-conotoxins (the arrangement of cysteine residues and a conserved arginine believed to interact with residues near the channel pore), it has distinctive features such as the absence of hydroxyproline. In voltage-clamped dissociated neurons from frog sympathetic and dorsal root ganglia, the peptide inhibited the majority of tetrodotoxin-resistant sodium currents irreversibly; in contrast, tetrodotoxin-sensitive sodium currents were largely unaffected by the peptide. We believe that μ-conotoxin SmIIIA is the first specific antagonist of tetrodotoxin-resistant voltage-gated sodium channels to be discovered. Thus, the peptide provides a new and potentially useful tool to investigate the functional roles of tetrodotoxin-resistant voltage-gated sodium channels, including those that are found in sensory nerves that convey nociceptive information.

Voltage-gated sodium channels (VGSCs)[1] are responsible for the influx of Na^+ during action potentials in excitable tissues. Molecular characterization of VGSCs has provided considerable insight into their structures, and thus far nine isotypes of the principal α-subunit of VGSCs have been cloned from mammals [see reviews by Catterall (*1*), Goldin (*2*), and Hille (*3*)].

A standard diagnostic pharmacological agent employed to investigate sodium channels is the classical blocker tetrodotoxin (TTX) (*4*), and sodium channels can be broadly classified as being either TTX-sensitive or TTX-resistant. However, both classes of channels comprise multiple molecular isoforms. Although gene knock-out and knock-down approaches have provided insights into the roles of specific VGSCs (*5*−*8*), a major impediment to investigating the physiology and biology of given sodium channel subtypes has been the lack of pharmacological agents that discriminate between the various channel isoforms.

Promising in this regard are μ-conotoxins from the venoms of predatory cone snails. The first μ-conotoxin characterized, μ-conotoxin GIIIA from *Conus geographus*, was shown to be much more specific than either of the guanidinium toxins TTX and saxitoxin (*9*). Like the latter toxins, μ-conotoxin GIIIA causes paralysis when injected into vertebrates; indeed, both μ-conotoxin and the guanidinium neurotoxins compete for binding to the same locus on the skeletal muscle sodium channel [see review by Cestele and Catterall (*10*)]. However, in contrast to TTX and saxitoxin, μ-conotoxin GIIIA selectively targets only one TTX-sensitive VGSC α-subunit isoform, the skeletal muscle subtype, μ1 or $Na_V1.4$, and this conotoxin has not been reported to inhibit any other VGSC subtype. A second μ-conotoxin, PIIIA, from a different venomous cone snail, *Conus purpurascens*, also strongly prefers the skeletal muscle subtype but can bind and inhibit some other TTX-sensitive subtypes as well, albeit with decreased affinity (*11*, *12*).

TTX-resistant VGSCs are of particular interest at the present time, but they suffer from a paucity of pharmacological agents that target them. We report here the characterization of a novel peptide from the fly speck cone, *Conus stercusmuscarum*, and demonstrate that this peptide, μ-conotoxin SmIIIA, inhibits TTX-resistant sodium channels in frog neurons with high affinity, as judged by its essentially irreversible action. This makes μ-conotoxin SmIIIA a unique ligand for VGSCs.

EXPERIMENTAL PROCEDURES

Isolation of μ-Conotoxin cDNAs from C. stercusmuscarum. Venom ducts were dissected from living snails, immediately frozen on dry ice, and stored at −80 °C. Venom duct tissue (∼100 mg) was homogenized and RNA extracted using TriReagent (MRC, Inc.) following standard protocols (*13*). Venom duct total RNA was used for cDNA synthesis primed with an oligo(dT) adapter primer [Lib-U primer: AAGCTCGAGTAACAACGCAGAGTAC$(T)_{20}$ NN] to facilitate 3′ RACE procedures. For PCR amplification of μ-conotoxin

† This work was supported by National Institute of General Medical Sciences Grant GM 48677.

* Corresponding author: telephone, (801) 581-3084; fax, (801) 585-5010; e-mail, yoshikami@biology.utah.edu.

‡ Interdepartmental Program in Neuroscience, University of Utah.

§ Department of Biology, University of Utah.

|| Cognetix, Inc.

[1] Abbreviations: DRG, dorsal root ganglion; MTBE, methyl *tert*-butyl ether; TTX, tetrodotoxin; VGSC, voltage-gated sodium channel.

10.1021/bi0265628 CCC: $22.00 © 2002 American Chemical Society
Published on Web 11/22/2002

genes, 5′ forward primers based on conserved propeptide regions of previously isolated μ-family genes were used in conjunction with the Lib-U adapter primer for 3′ RACE amplification of *C. stercusmuscarum* venom duct cDNA. PCR amplifications were performed with a cycling protocol consisting of an initial denaturation of 95 °C for 30 s followed by 30 cycles of 95 °C for 10 s, 56 °C for 10 s, and 72 °C for 30 s, concluding with a final extension at 72 °C for 10 min. Amplifications were done using *Taq* polymerase and standard reaction conditions, and PCR products were analyzed by electrophoresis on 2% agarose gels. Amplification of *C. stercusmuscarum* venom duct cDNA generated a prominent PCR product of ~400 bp. This product was gel-purified and Topo-TA cloned into the vector pCR-2.1 (Invitrogen). Transformed colonies were screened for inserts with the appropriate ~400 bp size, and multiple colonies were selected for DNA sequence analysis. Analysis of the cDNA sequences identified the open reading frames encoding the complete precursor protein for μ-conotoxins.

Synthesis and Folding of μ-Conotoxin SmIIIA. Peptides were synthesized using standard solid-phase Fmoc protocol and standard side chain protections. The polypeptides were cleaved from the solid support by exposure to reagent K (TFA/water/ethanedithiol/phenol/thioanisole, 90/5/2.5/7.5/5 by volume) for 8 h at room temperature. The crude peptide was precipitated with cold methyl *tert*-butyl ether (MTBE) and washed several times with cold MTBE. The linear form was purified using semipreparative reversed-phase C_{18} HPLC. The identity of the linear polypeptide was confirmed by electrospray ionization mass spectrometry. Folding reactions were carried out at room temperature and contained 0.1 M Tris-HCl, 0.1 mM EDTA, 1 mM GSSG, 1 mM GSH, pH 8.7, and 20−50 μM linear polypeptide. After 1 h, the folding reaction was quenched by adding formic acid to a final concentration of 5%. The reaction mixture was separated by reversed-phase C_{18} HPLC with a linear gradient of acetonitrile in 0.1% TFA from 9% to 31.5% in 20 min. For analytical and semipreparative C_{18} columns, flow rates of 1 and 5 mL/min were used, respectively. All HPLC chromatography was monitored using absorbance at 220 nm.

Neuronal Preparation and Electrophysiology. Lumbar sympathetic ganglia and dorsal root ganglia (DRG) were dissected from 2.5 to 3 in. *Rana pipiens* and processed in a manner similar to that described by Jones (*14*) and Campbell (*15*). Briefly, ganglia were treated with collagenase followed by trypsin. Cells were mechanically dissociated by trituration, washed and suspended in 73% Leibowitz's L15 solution (supplemented with 14 mM glucose, 1 mM $CaCl_2$, 7% fetal bovine serum, and penicillin/streptomycin), plated on poly-lysine-coated coverslips, and stored at 4 °C.

Whole cell recordings were carried out at room temperature with an Axopatch 200B amplifier (Axon Instruments). Neurons were perfused with extracellular solution containing (in mM) NaCl, 117; KCl, 2; $MgCl_2$, 2; $MnCl_2$, 2; HEPES, 5; and TEA, 10; pH 7.2. Recording pipets contained (in mM) NaCl, 10; CsCl, 110; $MgCl_2$, 2; $CaCl_2$, 0.4; EGTA, 4.4; HEPES, 5; TEA, 5; and MgATP, 4; pH 7.2. These solutions inhibit voltage-gated potassium and calcium currents and thereby permit recording of voltage-gated sodium currents exclusively. Conotoxins were dissolved in extracellular solution and applied to neurons under study by bath exchange. Toxin exposures were conducted in static baths.

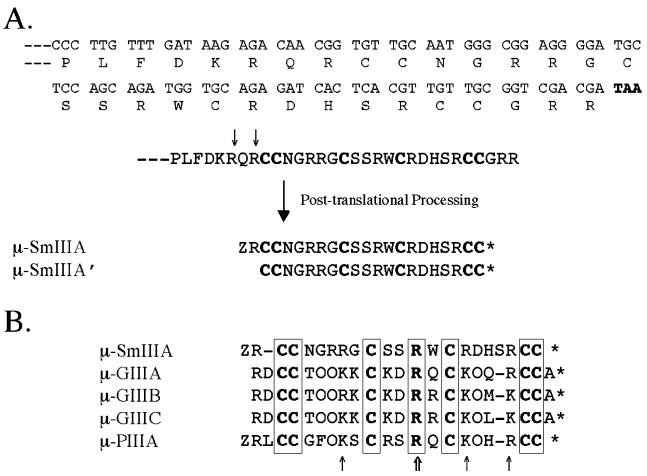

FIGURE 1: Sequence of cDNA clone Sm3.3 and the predicted peptides it encodes (panel A) and comparison with previously described μ-conotoxins (panel B). (A) cDNA clone Sm3.3 obtained from the venom duct of *C. stercusmuscarum* with the corresponding amino acid sequence of the encoded open reading frame (C-terminal 31 amino acids only). The initial translation product is posttranslationally processed: proteolytic digestion at the loci shown by arrows; conversion of the C-terminal ...CCGRR sequence to ...CC-NH_2 by the C-terminal amidation enzyme (blocked C-termini are represented by asterisks); and in the case of μ-SmIIIA, conversion of glutamine to pyroglutamate by a cyclase after proteolytic digestion. All of these posttranslational modifications are standard for many neuropeptides. Proteolytic cleavage at the left and right arrows yields μ-conotoxin SmIIIA and μ-conotoxin SmIIIA′, respectively. (B) Comparison of the sequence of μ-conotoxin SmIIIA to those of previously characterized μ-conotoxins which are highly selective for skeletal muscle VGSCs. Residues common to all toxins are boxed. μ-Conotoxins GIIIA, GIIIB, and GIIIC are from *C. geographus*, while μ-conotoxin PIIIA is from *C. purpurascens*. Key: O, hydroxyproline; Z, pyroglutamate; light arrows, conserved basic residues; bold arrow, conserved Arg residue.

To evoke voltage-gated Na currents, the neuron was held at −80 mV while 50 ms test pulses to 0 mV were applied every 5−10 s. Each test pulse was preceded by a −120 mV prepulse lasting 50 ms to relieve steady-state inactivation. Current signals were filtered at 2 kHz, digitized at 10 kHz, and leak-subtracted by a P/5 protocol using homemade software written in LabVIEW (National Instruments). Data were analyzed with Graphpad Prism for Macintosh (version 3.0cx, Graphpad Software). Data are presented as mean ± SEM, and error bars on all graphs are SEM.

RESULTS

Cloning and Chemical Synthesis of μ-Conotoxin SmIIIA. The nucleotide sequence of a cDNA clone (Sm3.3) obtained from the venom duct of the fly speck cone, *C. stercusmuscarum*, indicated that it encoded a peptide belonging to the μ-conotoxin family (Figure 1). The predicted final mature gene product after posttranslational modification is shown in Figure 1B along with the sequences of four previously characterized μ-conotoxins. The mature peptide shares several features with previously characterized μ-conotoxins; both the arrangement of cysteine residues and one arginine residue (R13) are conserved in all five sequences. The conserved Arg residue (bold arrow in Figure 1B) is known to be essential for biological activity in other μ-conotoxins and was postulated to be close to the extracellular opening of the sodium channel pore when the peptide is blocking its

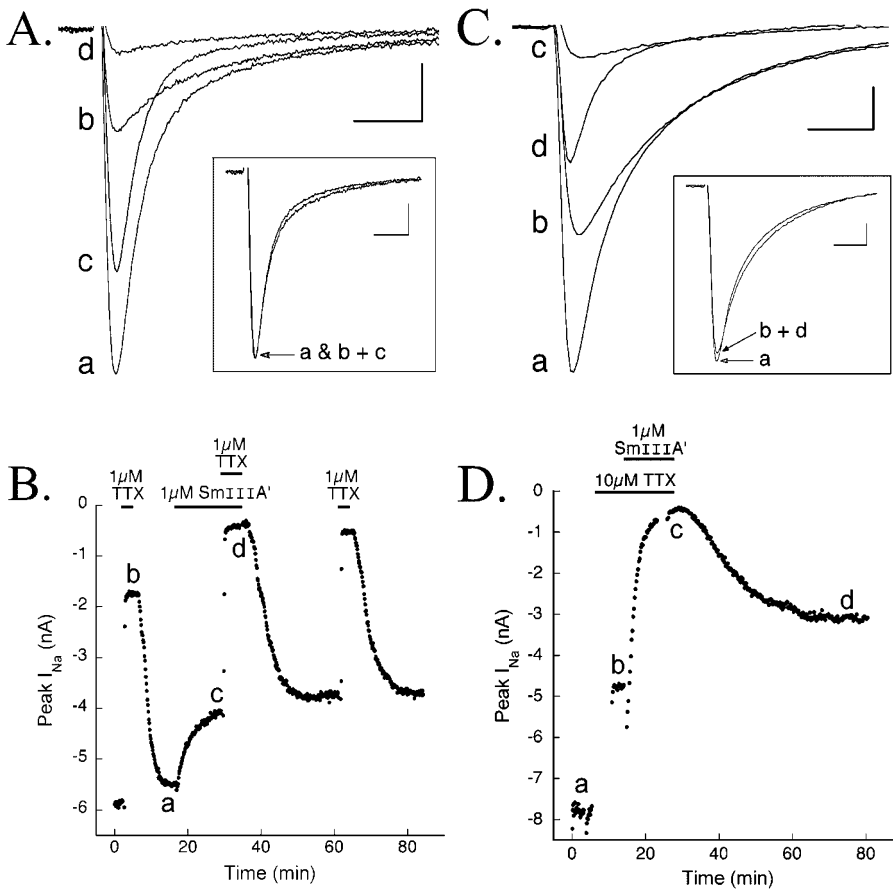

FIGURE 2: μ-Conotoxin SmIIIA′ irreversibly blocks TTX-resistant Na currents in a sympathetic neuron (panels A and B) and a sensory neuron (panels C and D). Neurons were prepared and whole-cell voltage-clamped as described in Experimental Procedures. Neurons were held at −80 mV while 50 ms test pulses to 0 mV were applied every 5−10 s. Each test pulse was preceded by a −120 mV prepulse lasting 50 ms to relieve steady-state inactivation. (A) Representative Na currents produced when command voltage was stepped to 0 mV in the presence of (a) control solution, (b) 1 μM TTX, (c) 1 μM SmIIIA′, and (d) 1 μM TTX + 1 μM SmIIIA′. The TTX-resistant current (trace b) was digitally added to the SmIIIA′-resistant current (trace c), and the resultant trace is shown in the inset along with the control current (trace a); the two traces essentially superimpose, suggesting that the SmIIIA′-resistant current is the TTX-sensitive current. (B) Peak Na current amplitudes (I_{Na}) plotted as a function of time. The presence of TTX and/or SmIIIA′ in the bath are (is) indicated by black bars. Responses averaged for the illustration in panel A were taken from those locations labeled with corresponding lower case letters. Note that the amount of the TTX-resistant current coincides with the amount of SmIIIA′-sensitive current. (C) Each trace represents the average of 10 responses when command voltage was stepped to 0 mV in the presence of (a) control solution, (b) 10 μM TTX, (c) 10 μM TTX + 1 μM SmIIIA′, and (d) control solution during wash. Note that the current following wash (trace d) inactivates faster than the TTX-resistant current (trace b). The TTX-resistant current (trace b) and the wash current (trace d) were digitally added, and the resulting trace is shown in the inset along with the control current (trace a); similarity of the two traces suggests that the current during washing is the TTX-sensitive current. (D) Peak Na current amplitudes plotted as a function of time. The presence of TTX alone or with SmIIIA′ in the bath is indicated by black bars. Responses averaged for illustration in panel C were taken from those locations labeled with corresponding lower case letters. Note that the amplitude of the control current that is blocked by TTX is the same as that which remains following washout of SmIIIA′ + TTX, suggesting that the only current that recovers following wash is a TTX-sensitive current. Calibration scale, 1 nA × 2 ms for all.

sodium channel target (*11*, *16*, *17*). Additionally, there are three loci where, although the residues are not identical, a positively charged amino acid is always present (light arrows).

The sequence derived from the cDNA clone was somewhat ambiguous as to which of two putative proteolytic processing sites is actually used to yield the mature peptide, so both of the predicted peptides were chemically synthesized and folded as described in Experimental Procedures. The longer peptide, with glutamine as the first amino acid, is predicted to be blocked at the N-terminal end with a pyroglutamate residue after posttranslational processing through the activity of a cyclase (*18*). If cleavage occurred at the arginine immediately before the first cysteine residue, then a peptide shorter by two residues would be produced. When tested for functional activity (see next section), no significant differences between the two possible final gene products were discerned. We refer to the longer peptide as μ-conotoxin SmIIIA and the shorter peptide as μ-conotoxin SmIIIA′.

Electrophysiological Characterization. Dissociated neurons from sympathetic and dorsal root ganglia of frog were examined by whole-cell voltage clamp. Recordings in Figure 2 are representative of a series of experiments that demonstrate specific and irreversible inhibition of TTX-resistant sodium currents by μ-conotoxin SmIIIA′ in these neurons. Similar results were obtained for SmIIIA (not illustrated). The similarity of both peptides is further supported by their kinetics, as presented later (see Figure 3).

Sympathetic neurons have both TTX-sensitive and TTX-resistant Na currents (Figure 2A). Upon exposure to TTX,

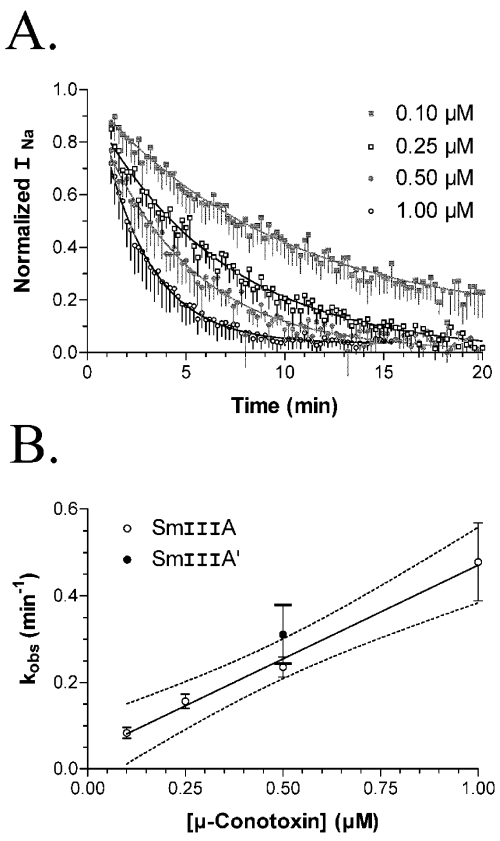

FIGURE 3: Rate of block of TTX-resistant I_{Na} as a function of SmIIIA concentration. Sympathetic neurons were prepared and whole-cell voltage-clamped as described in Experimental Procedures and Figure 2. (A) Time course of peak Na current inhibition by SmIIIA in the presence of 10 μM TTX. Peak responses in each trial were normalized, and the data points represent the averages of several trials at the following SmIIIA concentrations: 0.10 μM (closed squares, $N = 4$), 0.25 μM (open squares, $N = 6$), 0.50 μM (closed circles, $N = 6$), or 1.00 μM (open circles, $N = 5$). SmIIIA addition began at time 0 and bath exchange was complete within 1 min. Error bars represent SEM. Solid lines represent single exponential curve fits of averaged data starting from $t = 1$ min. (B) k_{obs} versus concentration of SmIIIA (open circles) or SmIIIA′ (single closed circle). Data used in panel B are the same as used in panel A; however, k_{obs} points are means determined from the single exponential best fits of individual trials at each toxin concentration, as opposed to the best fit of the averaged data as illustrated in panel A. Thus, each point represents the mean $k_{obs} \pm$ SEM (in min^{-1}) which are as follows: 0.08 ± 0.01 ($N = 4$), 0.16 ± 0.02 ($N = 6$), 0.24 ± 0.02 ($N = 6$), and 0.48 ± 0.09 ($N = 5$) for 0.10, 0.25, 0.50, and 1.00 μM SmIIIA, respectively, and 0.31 ± 0.11 ($N = 3$) for 0.5 μM SmIIIA′. The latter value suggests that the kinetics of SmIIIA′ is similar to that of SmIIIA. The best-fit linear regression line (solid curve) and 95% confidence interval (dashed curves) are shown for SmIIIA. The slope of this line is 0.43 ± 0.07 μM^{-1}·min^{-1}, and its Y-intercept is 0.04 ± 0.04 min^{-1}.

the current that remained had distinctly slower inactivation kinetics. After washing out TTX, the current essentially returned to its former amplitude (Figure 2B).

Addition of μ-conotoxin SmIIIA′ resulted in a diminution of the total Na current, and the current that persisted in the presence of the μ-conotoxin was more rapidly inactivating than the TTX-resistant current. When the TTX-resistant and the SmIIIA′-resistant currents are digitally summed, the original current is obtained (see Figure 2A, inset). Addition of TTX after SmIIIA′ was applied produced almost total inhibition of the inward current. After a second round of washing, only the component inhibited by TTX returned, and the current amplitude observed after the final wash was essentially that observed in the presence of SmIIIA′ alone, indicating that the effects of SmIIIA′ are irreversible over the time course of this experiment (Figure 2B).

As shown in Figure 2C,D, the effects of μ-conotoxin SmIIIA′ on sensory neurons from dorsal root ganglia (DRG) were similar to those observed for sympathetic neurons. However, as shown in Figure 2C, a larger proportion of the total Na current was TTX-resistant (>50% in this DRG neuron vs <30% in the sympathetic neuron). Addition of μ-conotoxin SmIIIA′ inhibited the current that persisted in TTX, and when both toxins were washed out, a more rapidly inactivating component of the Na current reappeared (see trace d in Figure 2C). When both the TTX-resistant and wash components were digitally summed, the original total current was essentially reconstituted, which suggests that the current recovered after washout of TTX and SmIIIA′ is only the TTX-sensitive current (see inset to Figure 2C). Thus, as with sympathetic neurons, μ-conotoxin SmIIIA′ appears to inhibit the TTX-resistant current in sensory neurons irreversibly.

In Figure 2, the residual current that seems to persist in the presence of both TTX and SmIIIA′ is the result of prematurely washing away the toxin; when the data are fit by a single exponential decay function, the predicted plateau indicates that the block had not yet reached steady state. This is consistent with the observation that, when normalized to one another, the residual current's waveform (Figure 2A, trace d, and Figure 2C, trace c) is the same as that of the TTX-resistant current before exposure to SmIIIA′ (Figure 2A, trace b, and Figure 2C, trace b) (normalized traces not shown); furthermore, in other experiments, this residual current was eventually totally abolished by more prolonged toxin exposures.

Since the toxin blocks TTX-resistant Na currents irreversibly over the time course of these experiments (no recovery observed when washed for 30 min), it was not possible to determine its IC_{50}; instead, the kinetics of inhibition were examined (Figure 3). Neurons were first exposed to 10 μM TTX; then the bath was flushed with a solution containing both 10 μM TTX and SmIIIA such that the bath exchange, which began at time zero in Figure 3A, was complete within 1 min. The block of TTX-resistant sodium currents by SmIIIA followed a single exponential decay curve whose rate increased with increasing peptide concentration (Figure 3A). This relationship was quantitatively assessed by plotting the observed rate constants (k_{obs}'s) as a function of toxin concentration (Figure 3B). The k_{obs} for each peptide concentration was obtained as follows: (1) normalizing the curves of all trials at that concentration, (2) fitting each to a single exponential, and then (3) averaging the best-fit rate constants. The slope of the linear regression line in Figure 3B is 0.43 ± 0.07 μM^{-1}·min^{-1} (or $0.7 \pm 0.1 \times 10^4$ M^{-1}·s^{-1}), and the extrapolated Y-intercept is close to zero (0.04 ± 0.04 min^{-1}). These results are consistent with a one to one interaction between the toxin and its receptor site on the TTX-resistant sodium channel, whose kinetics is described by the equation $k_{obs} = k_{on}[\text{toxin}] + k_{off}$. The predicted k_{off} close to zero is consistent with the experimental observation that the block produced by toxin is essentially irreversible.

As indicated earlier, SmIIIA and SmIIIA′ behave similarly. To determine their relative abilities to block the TTX-resistant sodium currents in sympathetic neurons, their

kinetics of block were compared. At a concentration of 0.5 μM, SmIIIA′ blocked with a $k_{obs} = 0.31 \pm 0.11$ min^{-1} ($N = 3$; see filled circle in Figure 3B). This value is statistically the same as the k_{obs} of 0.5 μM SmIIIA, 0.24 ± 0.02 min^{-1} ($N = 6$; open circle in Figure 3B) (where significant difference is determined at $p < 0.05$, unpaired t test).

We conclude that there are at least two different major sodium currents in both dissociated sympathetic and DRG neurons: one is TTX-resistant but sensitive to μ-conotoxin SmIIIA, and the other is TTX-sensitive but μ-SmIIIA-resistant. The μ-conotoxin blocks the TTX-resistant current irreversibly over the time course of these experiments, while TTX blocks the μ-SmIIIA-resistant current reversibly.

DISCUSSION

Recently, there has been considerable interest in TTX-resistant VGSCs because they, along with TTX-sensitive VGSCs, are found in sensory neurons that convey nociceptive (or pain) information (*19*−*21*). However, there are no reagents that have heretofore been developed that allow a pharmacological dissection of this class of channels.

Our electrophysiological experiments were performed on neurons from sympathetic and dorsal root ganglia of frog. The results confirm previous reports that neurons from these ganglia have both TTX-resistant and TTX-sensitive Na currents, with the former having slower inactivation kinetics than the latter (*14*, *15*). Likewise, it has been known since their initial characterization that TTX-resistant Na currents in mammalian (rat) DRG neurons inactivate more slowly than their TTX-sensitive counterparts (*22*). The IC_{50} for TTX is in the range of 10 nM for TTX-sensitive channels from both frogs (*14*) and mammals (*2*). In contrast, the IC_{50} is 3 orders of magnitude larger for TTX-resistant channels from both frogs (*14*) and mammals: the latter have two isotypes of TTX-resistant VGSC α-subunits, $Na_V1.8$ ($IC_{50} \sim 50-100$ μM) (*23*, *24*) and $Na_V1.9$ ($IC_{50} \sim 40$ μM) (*20*, *25*). Although VGSCs from an assortment of animal species have been cloned (for review see ref *26*), none from frog appears to have been cloned thus far, and it remains to be seen how similar, at a molecular level, the TTX-resistant VGSCs investigated in this report are to those in mammals. It might be noted that, in DRG of both frogs (*15*) and mammals (*19*), TTX-resistant channels are found predominantly in small diameter neurons, and it has long been appreciated that nociceptive signals in the periphery of both frogs and mammals are conveyed by slow-conducting sensory axons (*27*).

Our data establish that a new μ-conotoxin from the fly speck cone, *C. stercusmuscarum*, preferentially blocks TTX-resistant Na currents in neurons. We believe this is the first antagonist of VGSCs with this specificity to be discovered. This peptide, μ-conotoxin-SmIIIA/SmIIIA′, was discovered by cloning. Although neither SmIIIA nor SmIIIA′ has been purified from venom yet, homologous peptides purified from venom have, like SmIIIA, the N-terminal pyroGlu·Arg (G. Bulaj, unpublished). This leads us to suspect that SmIIIA is the native form of the conotoxin. In any event, both SmIIIA and SmIIIA′ were synthesized and shown to possess similar affinities for TTX-resistant sodium currents in frog neurons (Figure 3B). We will not distinguish between the two forms of the peptide for the remainder of this discussion.

μ-Conotoxin-SmIIIA has a strikingly different spectrum of subtype selectivity for VGSCs compared to the previously characterized μ-conotoxins (e.g., μ-conotoxins GIIIA, GIIIB, and GIIIC from *C. geographus* and μ-conotoxin PIIIA from *C. purpurascens*). All previously characterized μ-conotoxins have a strong preference for the $Na_V1.4$ subtype expressed in skeletal muscle, and it is likely that these are part of the "motor cabal" of toxins that fish-hunting cone snails have evolved to interfere with neuromuscular transmission (*28*). We have observed that neither μ-conotoxin GIIIA nor PIIIA inhibits TTX-resistant Na currents in frog sympathetic neurons (unpublished results), just as Nielsen et al. have recently reported that μ-conotoxin PIIIA does not block TTX-resistant currents in rat sensory neurons (*29*). It might be noted that there are other μ-conotoxins found in *C. stercus-muscarum* venom, including peptides that appear to have the same specificity as μ-conotoxins GIIIA or PIIIA (G. Bulaj, J. Garrett, M. Watkins, and B. Olivera, unpublished).

In some neurons, there was a minor residual current resistant to both TTX and SmIIIA which had even slower inactivation kinetics than the TTX-resistant but SmIIIA-sensitive current (data not shown). Furthermore, sympathetic neurons in some preparations had an additional TTX-sensitive current that was reversibly blocked by μ-conotoxin SmIIIA (data also not shown). These sporadically seen currents are absent in the cells shown in Figure 2 and are under further investigation.

It is clear that SmIIIA irreversibly inhibits the major TTX-resistant Na currents. This result is of potential biomedical importance, given that TTX-resistant VGSCs are considered to be promising molecular targets for new anesthetics and analgesics (*19*, *30*).

The k_{on} for SmIIIA estimated from the slope of the plot in Figure 3B is 0.7×10^4 M^{-1}·s^{-1}, a value slightly lower than the k_{on} reported for the block of exogenously expressed rat $Na_V1.4$ by μ-conotoxin GIIIA (6.1×10^4 M^{-1}·s^{-1}) or GIIIB (2.2×10^4 M^{-1}·s^{-1}) (*31*). A comparison of the sequence of SmIIIA with those of the previously characterized μ-conotoxins is shown in Figure 1B. Some of the typical characteristics of μ-conotoxins are clearly highly conserved. The arrangements of cysteine residues in the primary sequence, coupled with the presence of a conserved arginine residue, are some of the features shared by all of these peptides. However, there are a number of striking differences as well: for example, SmIIIA is the first member of the family lacking a hydroxyproline residue; all previously characterized peptides in the family have two to three residues of hydroxyproline. Some of these divergent sequence features are presumably important for the different spectrum of channel subtype selectivity observed with SmIIIA. Clearly, it will be of interest to elucidate what structural features of SmIIIA confer the novel specificity observed with this peptide for TTX-resistant sodium channels. Experiments to define such structure−function relationships are underway.

ACKNOWLEDGMENT

We thank Jake Nielsen for preparation of the synthetic peptides.

REFERENCES

1. Catterall, W. A. (2000) *Neuron 26*, 13−25.
2. Goldin, A. L. (2001) *Annu. Rev. Physiol. 63*, 871−894.

3. Hille, B. (2001) *Ion Channels in Excitable Membranes*, 3rd ed., Sinauer Associates, Sunderland, MA.
4. Narahashi, T., Moore, J. W., and Scott, W. R. (1964) *J. Gen. Physiol. 47*, 965−974.
5. Akopian, A. N., Souslova, V., England, S., Okuse, K., Ogata, N., Ure, J., Smith, A., Kerr, B. J., McMahon, S. B., Boyce, S., Hill, R., Stanfa, L. C., Dickenson, A. H., and Wood, J. N. (1999) *Nat. Neurosci. 2*, 541−548.
6. Khasar, S. G., Gold, M. S., and Levine, J. D. (1998) *Neurosci. Lett. 256*, 17−20.
7. Porreca, F., Lai, J., Bian, D., Wegert, S., Ossipov, M. H., Eglen, R. M., Kassotakis, L., Novakovic, S., Rabert, D. K., Sangameswaran, L., and Hunter, J. C. (1999) *Proc. Natl. Acad. Sci. U.S.A. 96*, 7640−7644.
8. Yoshimura, N., Seki, S., Novakovic, S. D., Tzoumaka, E., Erickson, V. L., Erickson, K. A., Chancellor, M. B., and de Groat, W. C. (2001) *J. Neurosci. 21*, 8690−8696.
9. Cruz, L. J., Gray, W. R., Olivera, B. M., Zeikus, R. D., Kerr, L., Yoshikami, D., and Moczydlowski, E. (1985) *J. Biol. Chem. 260*, 9280−9288.
10. Cestele, S., and Catterall, W. A. (2000) *Biochimie 82*, 883−892.
11. Shon, K. J., Olivera, B. M., Watkins, M., Jacobsen, R. B., Gray, W. R., Floresca, C. Z., Cruz, L. J., Hillyard, D. R., Brink, A., Terlau, H., and Yoshikami, D. (1998) *J. Neurosci. 18*, 4473−4481.
12. Safo, P., Rosenbaum, T., Shcherbatko, A., Choi, D. Y., Han, E., Toledo-Aral, J. J., Olivera, B. M., Brehm, P., and Mandel, G. (2000) *J. Neurosci. 20*, 76−80.
13. Chomczynski, P. (1983) *BioTechniques 15*, 532−535.
14. Jones, S. W. (1987) *J. Physiol. 389*, 605−627.
15. Campbell, D. T. (1992) *Proc. Natl. Acad. Sci. U.S.A. 89*, 9569−9573.
16. Becker, S., Prusak-Sochaczewski, E., Zamponi, G., Beck-Sickinger, A. G., Gordon, R. D., and French, R. J. (1992) *Biochemistry 31*, 8229−8238.
17. Sato, K., Ishida, Y., Wakamatsu, K., Kato, R., Honda, H., Ohizumi, Y., Nakamura, H., Ohya, M., Lancelin, J. M., Kohda, D., et al. (1991) *J. Biol. Chem. 266*, 16989−16991.
18. Craig, A. G., Bandyopadhyay, P., and Olivera, B. M. (1999) *Eur. J. Biochem. 264*, 271−275.
19. Baker, M. D., and Wood, J. N. (2001) *Trends Pharmacol. Sci. 22*, 27−31.
20. Dib-Hajj, S., Black, J. A., Cummins, T. R., and Waxman, S. G. (2002) *Trends Neurosci. 25*, 253−259.
21. Novakovic, S. D., Eglen, R. M., and Hunter, J. C. (2001) *Trends Neurosci. 24*, 473−478.
22. Kostyuk, P. G., Veselovsky, N. S., and Tsyndrenko, A. Y. (1981) *Neuroscience 6*, 2423−2430.
23. Akopian, A. N., Sivilotti, L., and Wood, J. N. (1996) *Nature 379*, 257−262.
24. Sangameswaran, L., Delgado, S. G., Fish, L. M., Koch, B. D., Jakeman, L. B., Stewart, G. R., Sze, P., Hunter, J. C., Eglen, R. M., and Herman, R. C. (1996) *J. Biol. Chem. 271*, 5953−5956.
25. Cummins, T. R., Dib-Hajj, S. D., Black, J. A., Akopian, A. N., Wood, J. N., and Waxman, S. G. (1999) *J. Neurosci. 19*, RC43.
26. Goldin, A. L. (2002) *J. Exp. Biol. 205*, 575−584.
27. Adrian, E. D. (1932) *Proc. R. Soc. London, Ser. B 109*, 1−18.
28. Olivera, B. M. (1997) *Mol. Biol. Cell 8*, 2101−2109.
29. Nielsen, K. J., Watson, M., Adams, D. J., Hammarstrom, A. K., Gage, P. W., Hill, J. M., Craik, D. J., Thomas, L., Adams, D., Alewood, P. F., and Lewis, R. J. (2002) *J. Biol. Chem. 277*, 27247−27255.
30. Julius, D., and Basbaum, A. I. (2001) *Nature 413*, 203−210.
31. Cummins, T. R., Aglieco, F., and Dib-Hajj, S. D. (2002) *Mol. Pharmacol. 61*, 1192−1201.

BI0265628